

Characteristic withdrawal capacity and stiffness of threaded rods

Haris Stamatopoulos and Kjell Arne Malo

Norwegian University of Science and Technology (NTNU), Trondheim, Norway

Keywords: Threaded rod, withdrawal capacity, withdrawal stiffness, embedment length, rod-to-grain angle, withdrawal strength parameter

1 Introduction

Long threaded rods show high withdrawal capacity and stiffness and thus they may be used in order to realize strong and stiff connections for timber structures. In comparison to dowel-type connectors, they have no initial soft response and no initial slip. In comparison to glued-in-rods they are less prone to construction quality issues, less brittle and offer greater protection against high temperatures (Mischler and Frangi 2001). Due to their length, their withdrawal capacity and stiffness are not significantly affected by local defects. Furthermore, a high degree of pre-fabrication is possible and hence easy and fast erection on site may be achieved.

Over the last years, the vast majority of the research effort has been devoted to the withdrawal capacity of screws with diameters up to 12 mm. The influence of parameters such as the embedment length and the angle between the screw axis and the grain direction has been investigated; see for example (Pirnbacher, Brandner and Schickhofer 2009, Frese and Blaß 2009). On the other hand, the research effort on the withdrawal capacity and also stiffness of threaded rods with diameters up to 20-25mm has not been so intensive and mostly it is limited to rods installed parallel and perpendicular to the grain (Jensen et al. 2011, Jensen et al. 2012, Nakatani and Komatsu 2004, Mori et al. 2008).

Eurocode 5, EC5 (CEN 2004) do not provide guidelines for the estimation of the withdrawal stiffness which is required for the evaluation of the stiffness of connections with threaded connectors (Tomasi, Crosatti and Piazza 2010, Malo and Ellingsbø

2010). Some expressions may be found in technical approvals of screws, but mostly these expressions are valid for screws with relatively small diameters. Moreover, EC5 does not allow the installation of rods in an angle to the grain less than 30° in order to eliminate the risk of splitting failure. However, in practice, it may be desired to install threaded rods in an angle to the grain smaller than 30° (in combination with some sort of reinforcement to prevent splitting failure).

In the present paper, an experimental study on withdrawal of threaded rods embedded in glue-laminated timber (abbr. glulam) elements is presented. The parameters of this study were the embedment length and the angle between the rod axis and the grain direction (with emphasis on angles which are smaller than 30°). Moreover, analytical expressions for the estimation of withdrawal capacity and stiffness are provided. The characteristic withdrawal capacity and the mean withdrawal stiffness were obtained by the experimental results and compared to the analytical estimations.

2 Experimental methods

2.1 Experimental set-up

The experimental set-up for the withdrawal tests is presented in Figure 1. As shown, the loading condition of the specimens was a 'remote' pull-push (i.e. the support was provided in the same plane surface as the entrance of the rod, but at a distance to the rod). A thin steel plate, as shown in Fig. 1d, was placed between the supports and the specimen. The plate was used to counteract bending stresses and prevent tensile splitting failure, while allowing local deformation on the surface of the specimen in the vicinity of the rod. Two displacement transducers were placed next to the supports of the specimen, measuring the relative displacement between the rod and support as shown in Figures 1a, 1c and 1e. The average of these two measurements was used for the displacement. Testing was performed using the loading protocol given in EN 26891:1991 (ISO6891:1983) (CEN 1991).

2.2 Materials

The specimens were cut from glulam beams of Scandinavian class L40c which corresponds to European strength class GL30c (CEN 2013). This type of glulam is fabricated with 45 mm thick lamellas, made of Norwegian spruce (*Picea Abies*). The mean and characteristic density of L40c is $\rho_{mean} = 470 \text{ kg/m}^3$ and $\rho_k = 400 \text{ kg/m}^3$ respectively. The mean moduli of elasticity, parallel and perpendicular to the grain, are $E_{0,mean} = 13000 \text{ MPa}$ and $E_{90,mean} = 410 \text{ MPa}$ respectively, and the shear modulus is $G = 760 \text{ MPa}$.

For increased homogeneity, all specimens were manufactured such that the rods were inserted in the inner, weaker lamellas of the beams. SFS WB-T-20 (DIBt 2010) steel threaded rods were used. These rods are made according to DIN7998 (DIN 1975). The outer-thread diameter d of the rods is 20 mm and the core diameter, d_c , is 15 mm. According to the manufacturer, the steel grade of the rods is 8.8 and their characteristic tensile capacity is 145 kN.

2.3 Specimens

Prior to rod installation, all specimens were pre-drilled with a diameter equal to d_c . All specimens were conditioned to standard temperature and relative humidity conditions (20°C / 65% R.H.), leading to approximately 12% moisture content in the wood. The parameters of the experimental investigation were the rod-to-grain angle, α , and the embedment length of the rod, l_{ef} . Specimens with 6 different rod-to-grain angles ($\alpha = 0, 10, 20, 30, 60$ and 90°) and 4 different embedment lengths ($l_{ef} = 100, 300, 450, 600$ mm) were tested. The series of specimens are denoted $S\alpha$ - l_{ef} , based on their rod-to-grain angle and embedment length. The width, b , of the glulam beams and consequently of all specimens was equal to 140 mm. A full description of the specimens' dimensions can be found in (Stamatopoulos and Malo 2015b).

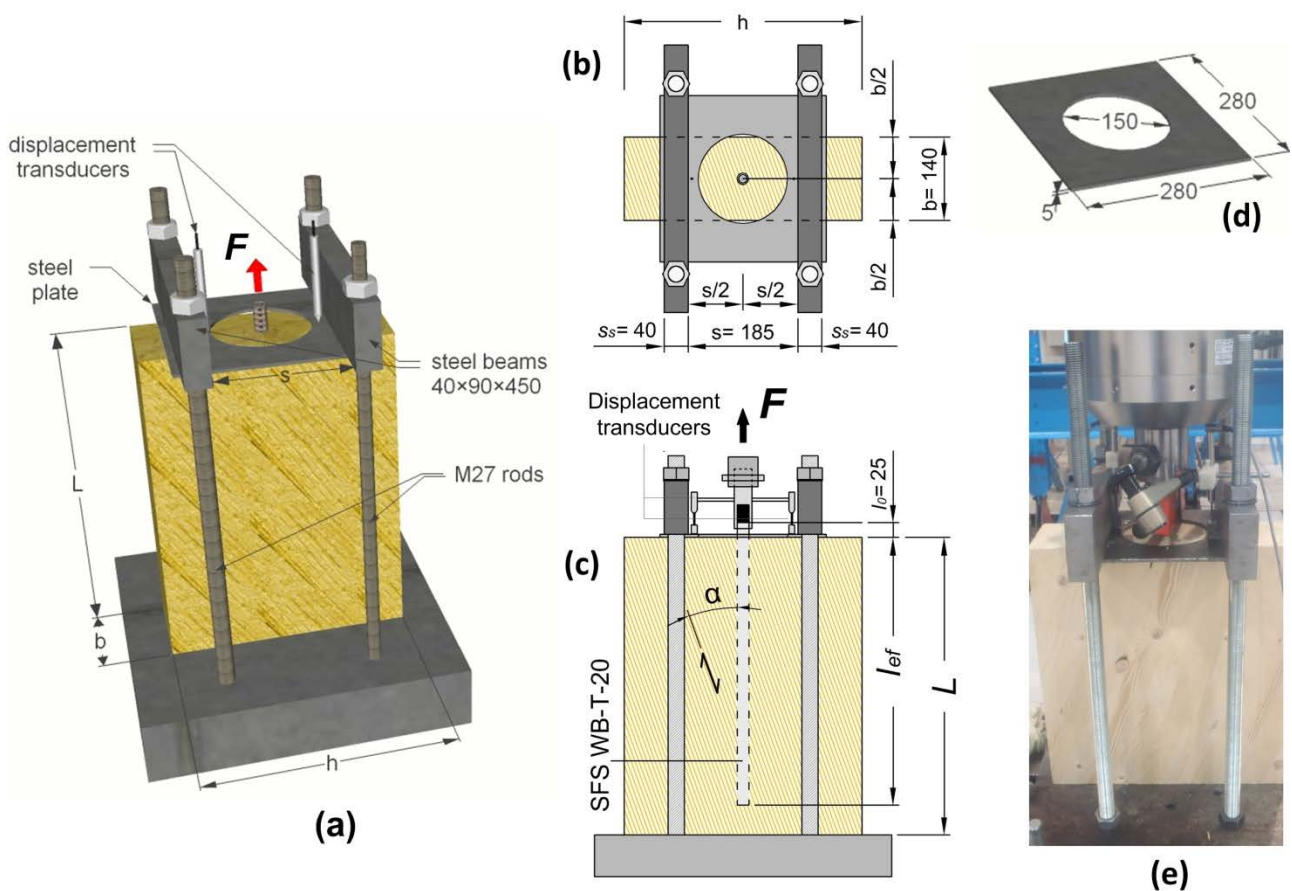


Figure 1. Experimental set-up: (a) 3D representation, (b) plan view, (c) side view, (d) steel plate and (e) photo

3 Eurocode 5

According to EC5 (for screws with $d > 12$ mm) the characteristic withdrawal capacity, $F_{ax.Rk}$, is given by (the expression is re-arranged):

$$F_{ax.Rk} = n_{ef} \cdot f_{ax.\alpha.k} \cdot d \cdot l_{ef} \quad (1)$$

The parameter n_{ef} is the effective number of screws and equal to $n_{ef} = n^{0.9}$, where n is the number of screws acting together in a connection. The withdrawal strength parameter, $f_{ax.\alpha.k}$, is given by:

$$f_{ax.\alpha.k} = \frac{f_{ax.90.k}}{1.2 \cdot \cos^2 \alpha + \sin^2 \alpha} \cdot \left(\frac{\rho_k}{\rho_a} \right)^{0.8} \quad (\alpha \geq 30^\circ) \quad (2)$$

where $f_{ax.90.k}$ is the withdrawal strength parameter perpendicular to the grain which must be experimentally determined, for the associated density ρ_a . EC5 provides no guidelines for the estimation of withdrawal stiffness.

In the technical approval of WB-T-20 rods, Z-9.1-777 (DIBt 2010), the following expression is provided for the withdrawal strength parameter (unit MPa and kg/m³):

$$f_{ax.k} = 70 \cdot 10^{-6} \cdot \rho_k^2 \quad (45^\circ \leq \alpha \leq 90^\circ) \quad (3)$$

4 Analytical model

Analytical estimations can be obtained by use of the concept of the classical Volkersen theory (Volkersen 1938), applied for axially loaded connectors (Jensen et al. 2001). This model has initially been developed assuming that all shear deformation occurs in an infinitely thin shear layer, while the connector and surrounding wood are assumed to be in states of pure axial stress. The shear stress-displacement behaviour ($\tau - \delta$) of the shear layer is approximated by a linear constitutive law, which is a reasonable approximation for glued-in-connectors.

In the case of screwed-in connectors, however, it is more convenient to assume a bi-linear constitutive law, because these connectors are by far less brittle than glued-in connectors and their post-elastic behaviour should not be omitted. The bi-linear constitutive law is presented in Figure 2. The bi-linear idealization separates the curve in two distinct domains; the linear elastic domain and the fracture domain. These domains are characterized by the equivalent shear stiffness parameters Γ_e and Γ_f , which are the slopes of the two branches of the bi-linear constitutive law. The advantage of this method is that, apart from the withdrawal capacity and stiffness, it also allows

the estimation stress and displacement distributions for any given withdrawal force level. Thus, an analytical estimation of the force-displacement curve can be obtained. Note that all shear deformation is assumed to occur in a shear zone of finite dimensions. A full description of this method is given in (Stamatopoulos and Malo 2015a).

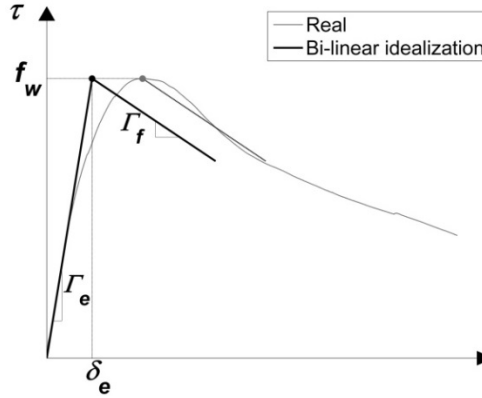


Figure 2. Bi-linear approximation of τ - δ curve

The withdrawal stiffness, K_w , and the characteristic withdrawal capacity, $F_{ax.Rk}$, are provided by the following expressions (Stamatopoulos and Malo 2015a, Jensen et al. 2001):

$$K_w = \pi \cdot d \cdot l_{ef} \cdot \Gamma_e \cdot \frac{\tanh \omega}{\omega} \quad (4)$$

$$\frac{F_{ax.\alpha.Rk}}{d \cdot l_{ef} \cdot f_{ax.\alpha.k}} = \frac{\sin(m \cdot \omega \cdot \lambda_u)}{\omega \cdot m} + \frac{\tanh\{(1 - \lambda_u) \cdot \omega\} \cdot \cos(m \cdot \omega \cdot \lambda_u)}{\omega} \quad (5)$$

Note that these expressions are valid for pull-push or pull-shear loading conditions, but not for the pull-pull loading condition. The parameter m has been introduced as:

$$m = \sqrt{\Gamma_f / \Gamma_e} \quad (6)$$

This parameter is a measure of the brittleness of the shear zone. In the limits, $m \rightarrow 0$ indicates perfect plastic post-elastic behaviour, while $m \rightarrow \infty$ indicates totally brittle behaviour. The parameters ω and β have been defined as follows:

$$\omega = \sqrt{\pi \cdot d \cdot \Gamma_e \cdot \beta \cdot l_{ef}^2} \quad (7)$$

$$\beta = \frac{1}{A_s \cdot E_s} + \frac{1}{A_w \cdot E_{w.\alpha}} \quad (8)$$

where E_s and $E_{w,\alpha}$ are the moduli of elasticity of steel and wood (as function of α), respectively. The core cross-sectional area of the rod is $A_s = \pi \cdot d_c^2/4$ and A_w is the area of wood subjected to axial stress. $E_{w,\alpha}$ may be estimated by the Hankinson formula and A_w by an effective area, confer (Stamatopoulos and Malo 2015b). The parameter λ_u is a dimensionless length parameter which expresses the percentage of the embedment length (at failure), in which post-elastic behaviour takes place and it can be determined by the diagram in Figure 3.

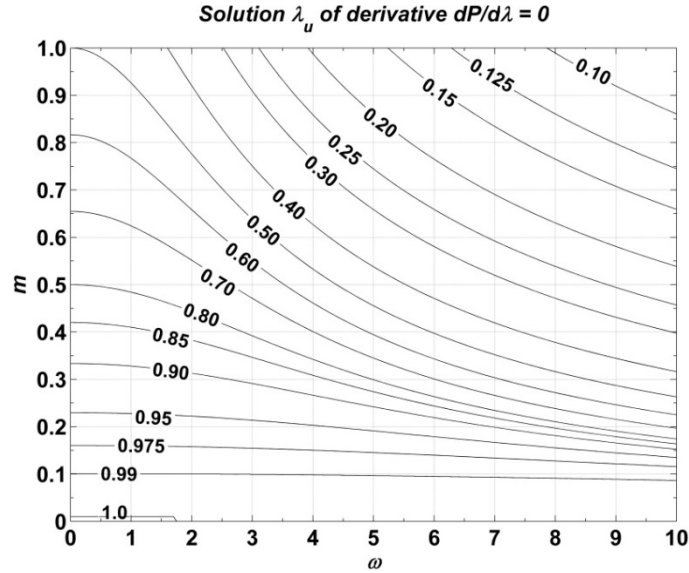


Figure 3. Diagram for the determination of parameter λ_u

The parameters Γ_e (in MPa/mm) and m are provided as functions of α , by the following expressions (Stamatopoulos and Malo 2015a):

$$\Gamma_{e,\alpha} = \frac{9.35}{1.5 \cdot \sin^{2.2} \alpha + \cos^{2.2} \alpha} \quad (9)$$

$$m_\alpha = \frac{m_0}{(m_0/m_{90}) \cdot \sin \alpha + \cos \alpha} = \frac{0.332}{1.73 \cdot \sin \alpha + \cos \alpha} \quad (10)$$

Finally, $f_{\alpha,\alpha,k}$ can be calculated by Equation (2).

5 Results and discussion

5.1 Withdrawal stiffness

The experimentally derived mean values of K_w and the coefficient of variation (abbr. C.o.V.) for all embedment lengths and rod-to-grain angles are summarized in Table 1. The sample size for each sub-set of parameters (l_{ef} and α) was 5 tests. The analytical

estimations are compared to the experimental results in Figure 4, where K_w is plotted as function of l_{ef} for all rod-to-grain angles. Results from finite element simulations are also provided in Figure 4. The finite element model has been presented in detail in (Stamatopoulos and Malo 2015b).

Table 1. Experimentally recorded mean withdrawal stiffness (units kN/mm) and C.o.V.

	$l_{ef}=100$ mm	$l_{ef}=300$ mm	$l_{ef}=450$ mm	$l_{ef}=600$ mm
	$K_{w.mean}$ /C.o.V.	$K_{w.mean}$ /C.o.V.	$K_{w.mean}$ /C.o.V.	$K_{w.mean}$ /C.o.V.
$\alpha = 0^\circ$	54.6 / 0.16	121.0 / 0.30	121.8 / 0.13	128.6 / 0.17
$\alpha = 10^\circ$	56.0 / 0.27	137.3 / 0.19	132.8 / 0.22	131.1 / 0.05
$\alpha = 20^\circ$	53.8 / 0.23	125.9 / 0.20	121.7 / 0.16	128.0 / 0.14
$\alpha = 30^\circ$	42.6 / 0.27	111.2 / 0.11	100.3 / 0.10	114.8 / 0.11
$\alpha = 60^\circ$	36.6 / 0.33	73.5 / 0.17	90.1 / 0.09	(-) ¹
$\alpha = 90^\circ$	29.0 / 0.31	61.4 / 0.11	66.6 / 0.16	(-) ¹

¹ Experiments were not performed for $l_{ef} = 600$ mm and $\alpha = 60^\circ, 90^\circ$

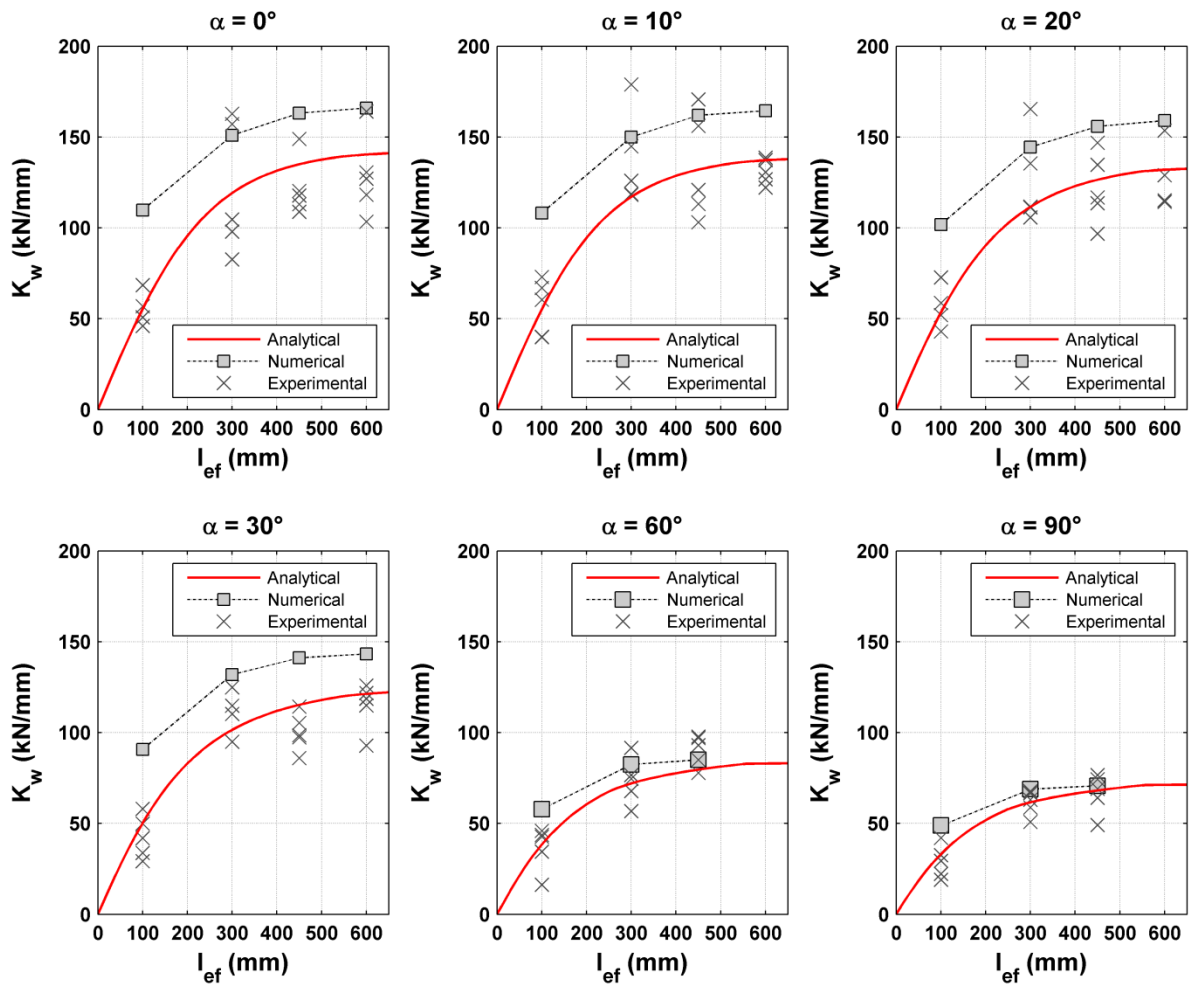


Figure 4. Withdrawal stiffness as function of l_{ef}

It is clear from the experimental results that the specimens exhibited high stiffness, especially for small rod-to-grain angles. As shown in Figure 4, the increase of withdrawal stiffness due to increasing embedment length becomes gradually smaller as the embedment length increases. This is estimated both analytically and by numerical results and validated experimentally. In fact, the experimental results for these threaded rods suggest that K_w has no correlation with the embedment length if $l_{ef} \geq 300$ mm. This is especially true for small rod-to-grain angles. Finally, according to experimental observations, no initial slip occurred if the threaded steel coupling parts of the set-up were tightly fastened.

5.2 Withdrawal strength parameter

The withdrawal strength parameter was calculated for all angles from the experimental results for all specimens. The mean values, the C.o.V., the median and the 5%-fractile characteristic values are provided in Table 2. It should be noted that the requirements of EN1382 (CEN 1999) for the determination of $f_{ax,\alpha}$ have not been met with respect to the embedment length and the edge distances. The characteristic values are calculated according to EN14358 (CEN 2006). In comparison to the experimental results presented in the previous Section, some additional experimental results have been used in Sections 5.2 and 5.3.

Table 2. Values of the withdrawal strength parameter $f_{ax,\alpha}$

	Number of tests	$f_{ax,\alpha} = F_{max} / d \cdot l_{ef}$ (MPa)			
		Mean	C.o.V.	Median	5% - fractile
$\alpha = 0^\circ$	25	13.81	0.152	13.79	10.19
$\alpha = 10^\circ$	22	14.14	0.168	13.90	10.06
$\alpha = 20^\circ$	20	15.70	0.145	16.05	11.46
$\alpha = 30^\circ$	20	15.16	0.136	15.52	11.47
$\alpha = 60^\circ$	16	15.17	0.124	15.75	11.50
$\alpha = 90^\circ$	20	14.88	0.108	15.04	11.92

* Note: the requirements of EN 1382 with respect to l_{ef} and the edge distances were not met for all specimens

The variability decreases with increasing angle. The ratio $f_{ax,90,k} / f_{ax,0,k}$ is equal to 1.17 which is very close to the ratio 1.20 according to Equation (2). Moreover, the withdrawal strength for rod-to grain angles 0° and 10° is significantly smaller than the withdrawal strength for greater angles. The experimental results together with the estimations by Equations (2) and (3) are presented in Figure 5.

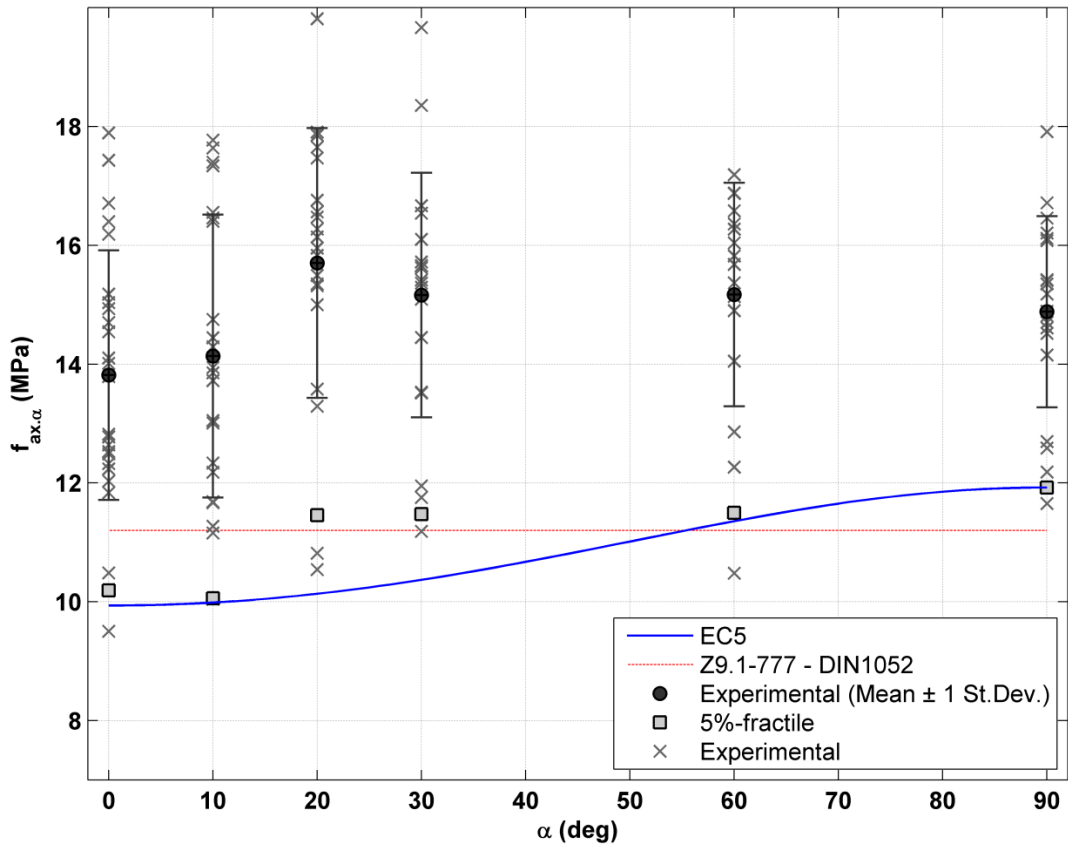


Figure 5. Withdrawal strength parameter as function of α

5.3 Withdrawal capacity

All specimens with $l_{ef} \leq 450$ mm failed due to withdrawal of the rod. In a few specimens with $l_{ef} = 450$ mm yielding of the rod was observed, however the increasing force due to steel hardening led to withdrawal failure prior to steel fracture. In the vast majority of the specimens with $l_{ef} = 600$ mm yielding of the rod was observed. All 5 specimens in S20-600 and S30-600 series and 3 out of 5 specimens in S10-600 series failed due to steel fracture (none in the S0-600 series). These values have been excluded from the calculation of $f_{ax,\alpha}$ in the previous Section. Yielding and steel fracture of the rods occurred at load levels which were significantly higher than those predicted by the nominal yield and ultimate strength properties of steel. The observed increase in strength of the steel can probably be attributed to steel hardening due to thread rolling.

The mean experimentally recorded capacities and their C.o.V. as well as the characteristic capacity for all embedment lengths and rod-to-grain angles are summarized in Table 3. The characteristic capacities have also been calculated according to EN 14358. A minimum C.o.V equal to 0.05 was used to calculate the characteristic capacities, in cases where C.o.V. was smaller.

The experimentally recorded capacities, together with the EC5 and the analytical estimations are plotted as function of the embedment length for all rod-to-grain angles in Figure 6. The withdrawal strength parameter was determined by Equation (2) and

by setting $f_{ax.90.k} = 11.92$ MPa (from Table 2). Note that Equation (2) has been used also outside its valid range for α .

Table 3. Experimentally recorded withdrawal capacity for all specimens (in kN)

	$l_{ef} = 100$ mm (10 tests)	$l_{ef} = 300$ mm (5 tests)	$l_{ef} = 450$ mm (5 tests)	$l_{ef} = 600$ mm (5 tests)
	$F_{ax.Rm} / C.o.V. / F_{ax.Rk}$			
$\alpha = 0^\circ$	26.2 / 0.14 / 19.6	89.7 / 0.12 / 66.8	130.2 / 0.24 / 66.7	161.6 / 0.05 / 141.8
$\alpha = 10^\circ$	25.8 / 0.18 / 17.9	99.8 / 0.10 / 76.9	127.5 / 0.14 / 88.7	173.1 ^{1a} / (-) / (-)
$\alpha = 20^\circ$	30.2 / 0.19 / 19.5	98.7 / 0.11 / 74.3	145.8 / 0.06 / 124.7	175.7/0.01/155.3 ^{1b}
$\alpha = 30^\circ$	27.9 / 0.13 / 20.9	99.9 / 0.11 / 77.4	144.6 / 0.09 / 115.5	176.7/0.01/156.2 ^{1b}
$\alpha = 60^\circ$	28.7 / 0.17 / 18.3 ²	93.6 / 0.12 / 66.9	141.7 / 0.03 / 125.2	(-) ³
$\alpha = 90^\circ$	28.0 / 0.12 / 21.7	96.5 / 0.07 / 80.8	139.2 / 0.05 / 121.9	(-) ³

^{1a} Steel and withdrawal failures were observed and thus no characteristic capacity was calculated, ^{1b} Steel failure, characteristic value calculated with C.o.V.=0.05, ² 6 tests (instead of 10), have been performed for $l_{ef} = 100$ mm and $\alpha = 60^\circ$, ³ No experiments performed for $l_{ef} = 600$ mm and $\alpha = 60^\circ, 90^\circ$.

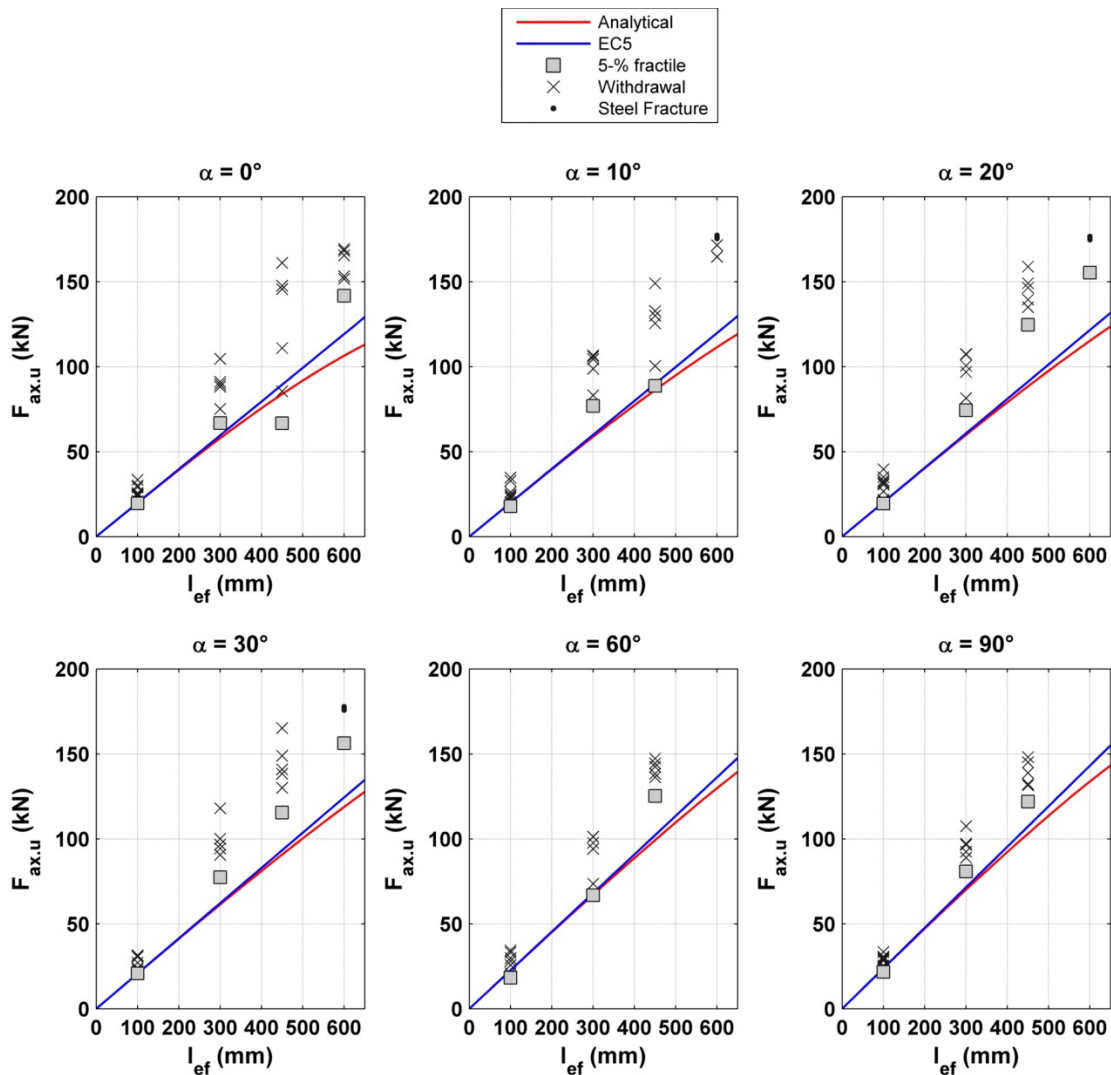


Figure 6. Withdrawal capacity as function of l_{ef}

As shown in Figure 6, Equation (5) results in a nearly linear relation between the capacity and the embedment length and thus the difference between Equations (1) and (5) is small. The estimations by Equations (1) and (5) are generally conservative, especially for $l_{ef} \geq 300$ mm and for $\alpha \geq 20^\circ$. According to the experimental results, the withdrawal capacity of specimens with $\alpha = 20^\circ$ was equally reliable as the capacity of specimens with greater angles. On the other hand, for $\alpha < 20^\circ$ the capacity may be less reliable like in series S0-450 where the evaluated from experiments characteristic capacity was smaller than the analytical prediction.

Finally, it has been reported (Ringhofer and Schickhofer 2014) that the long-term behaviour of axially loaded screws inserted parallel to the grain is very poor. It follows that the long-term behaviour of threaded rods (as function of the rod-to-grain angle and the embedment length) should be further explored.

6 Conclusions

The withdrawal of axially loaded threaded rods with a diameter of 20 mm, screwed into glulam was studied using experimental and analytical methods. The following main conclusions are drawn:

- The withdrawal stiffness and capacity can be estimated by use of a simple analytical procedure, based on the principle of Volkersen model.
- The characteristic withdrawal strength, as estimated by EC5 expression, is on the safe side especially for rod-to grain angles 20° and 30° .
- The characteristic withdrawal strengths for rod-to grain angles 0° and 10° are significantly smaller than the strengths for greater angles.
- The capacity of specimens with a rod-to-grain angle equal to 20° was equally reliable as the capacity of specimens with greater angles.
- Experimental, analytical and numerical results suggest that the increase of withdrawal stiffness due to increasing embedment length becomes gradually smaller as the embedment length increases.
- According to experimental observation, initial slip did not occur when the steel coupling parts of the set-up were tightly fastened.
- Steel fracture of the rods occurred at load levels which were significantly higher than those predicted by the nominal yield and ultimate strength properties of steel.

7 Acknowledgements

The support by The Research Council of Norway (208052) and The Association of Norwegian Glulam Producers, Skogtiltaksfondet and the Norwegian Public Road Administration is gratefully acknowledged. The authors would like to acknowledge the contribution of students Joakim Troller and Roland Falk in the preparation of the experiments.

8 References

- CEN, European committee for standardization. 1991. EN 26891:1991 (ISO 6891:1983): Timber structures- Joints made with mechanical fasteners-General principles for the determination of strength and deformation characteristics. Brussels, Belgium.
- CEN, European committee for standardization. 1999. EN 1382-1999: Timber structures- - Tests methods - Withdrawal capacity of timber fasteners. Brussels, Belgium.
- CEN, European committee for standardization. 2004. EN 1995-1-1:2004: Design of timber structures. Part 1-1: General-Common rules and rules for buildings. Brussels, Belgium.
- CEN, European committee for standardization. 2006. EN 14358-2006: Timber structures- Calculation of characteristic 5-percentile values and acceptance criteria of a sample. Brussels, Belgium.
- CEN, European committee for standardization. 2013. EN 14080-2013: Timber structures- Glued laminated timber and glued solid timber - Requirements. Brussels, Belgium.
- DIBt, Deutsches Institut für Bautechnik. 2010. SFS intec, GmbH., Gewindestangen mit Holzgewinde als Holzverbindungsmitel, Allgemeine bauaufsichtliche Zulassung Z-9.1-777.
- DIN, Deutsches Institut für Normung. 1975. DIN 7998:Gewinde und Schraubenenden für Holz-schrauben. Berlin, Germany.
- Frese, M. & H. J. Blaß. 2009. Models for the calculation of the withdrawal capacity of self-tapping screws. In *Proceedings of the 42nd CIB-W18 meeting* Dübendorf, Switzerland.
- Jensen, J. L., A. Koizumi, T. Sasaki, Y. Tamura & Y. Iijima (2001) Axially loaded glued-in hardwood dowels. *Wood Science and Technology*, 35, 73-83.
- Jensen, J. L., M. Nakatani, P. Quenneville & B. Walford (2011) A simple unified model for withdrawal of lag screws and glued-in rods. *European Journal of Wood and Wood Products*, 69, 537-544.

- Jensen, J. L., M. Nakatani, P. Quenneville & B. Walford (2012) A simplified model for withdrawal of screws from end-grain of timber. *Construction and Building Materials*, 29, 557-563.
- Malo, K. A. & P. Ellingsbø. 2010. On connections for timber bridges. In *Proceedings of the International Conference Timber Bridges (ICTB)*, 297-312. Lillehammer, Norway.
- Mischler, A. & A. Frangi. 2001. Pull-out tests on glued-in-rods at high temperatures. In *Proceedings of the 34th CIB-W18 meeting Venice, Italy*.
- Mori, T., M. Nakatani, S. Kawahara, T. Shimizu & K. Komatsu. 2008. Influence of the number of fastener on tensile strength of lagscrewbolted glulam joint. In *10th World Conference on Timber Engineering*, 1100-1107.
- Nakatani, M. & K. Komatsu. 2004. Development and verification of theory on pull-out properties of Lagscrewbolted timber joints. In *Proceedings of the 8th World Conference on Timber Engineering*, 95-99. Lahti, Finland.
- Pirnbacher, G., R. Brandner & G. Schickhofer. 2009. Base parameters of self-tapping screws. In *Proceedings of the 42nd CIB-W18 meeting Dübendorf, Switzerland*.
- Ringhofer, A. & G. Schickhofer. 2014. Influencing parameters on the experimental determination of the withdrawal capacity of self-tapping screws. In *Proceedings of the 13th World Conference on Timber Engineering*. Quebec City, Canada.
- Stamatopoulos, H. & K. A. Malo (2015a) Withdrawal capacity of threaded rods embedded in timber elements. *Construction and Building Materials*, 94, 387-397.
- Stamatopoulos, H. & K. A. Malo (2015b) Withdrawal stiffness of threaded rods embedded in timber elements. *Submitted to Construction and Building Materials*.
- Tomasi, R., A. Crosatti & M. Piazza (2010) Theoretical and experimental analysis of timber-to-timber joints connected with inclined screws. *Construction and Building Materials*, 24, 1560-1571.
- Volkersen, O. (1938) Die nietkraftverteilung in zugbeanspruchten nietverbindungen mit konstanten laschenquerschnitten. *Luftfahrtforschung*, 15, 41-47.